Spin dynamics of CeX_2Si_2 (X = Au, Pd, Rh, Ru)

A. Severing
II Physikalisches Institut der Universität zu Köln, Federal Republic of Germany and Institut Laue-Langevin, Grenoble, France

E. Holland-Moritz
Institut für Festkörperforschung, Kernforschungsanlage Jülich, Federal Republic of Germany and II Physikalisches Institut der Universität zu Köln, Federal Republic of Germany

B. Frick
Institut Laue-Langevin, Grenoble, France

(Received 27 June 1988)

The results of high-resolution inelastic neutron scattering experiments on CeX_2Si_2 (X=Au, Pd, Rb, and Ru) in the temperature interval 1.5–250 K are reported, and the interplay of $4f$ conduction-electron scattering and magnetic order is discussed. The quasielastic linewidths increase within the series $\Gamma/2(\mathrm{Au}) < \Gamma/2(\mathrm{Pd}) < \Gamma/2(\mathrm{Rh}) < \Gamma/2(\mathrm{Ru})$, although the Néel temperature of $CeRh_2Si_2$ is about four times larger than in the Au- and Pd-based compounds. The quasielastic linewidth of the nonordering compound $CeRu_2Si_2$ decreases linearly with temperature and converts into an inelastic line when the thermal energy becomes smaller than $\Gamma/2$. An analytic function given by Kuramoto and Müller-Hartmann is applied to fit the low-temperature data of $CeRu_2Si_2$. In addition, the low-temperature inelastic line in $CeRu_2Si_2$ exhibits a strong $|Q|$ dependence: its inelastic position and linewidth vary with $|Q|$.

INTRODUCTION

The current interest in materials of the type CeX_2Si_2 (X = transition-metal atom) may be attributed to the discovery of superconductivity in the heavy-fermion compound $CeCu_2Si_2$. Susceptibility and transport measurements have shown that an exchange of X from the middle of the transition metal row towards the noble metals results in a systematic change of the cerium valence from intermediate-valent (IV) to nearly trivalent. Some of the CeX_2Si_2 compounds also order magnetically. Therefore, the CeX_2Si_2 series provides a set of isostructural samples, ideally suited for studying the competition between the indirect exchange interaction of Ce^{3+} ions via the Ruderman-Kittel-Kasuya-Yosida (RKKY) oscillations and the effective surpression of the Ce^{3+} moments due to Kondo spin or valence fluctuations. The temperature T_{RKKY} and the Kondo temperature T_K measure the strength of the respective processes. The Kondo temperature T_K can be determined from the zero-temperature value of the quasielastic linewidth $\Gamma/2$ in the magnetic neutron scattering response. However, in the magnetically ordering compounds we determine T_K from the width of the quasielastic line at the ordering temperature.

In this paper we present results of high-resolution inelastic neutron scattering experiments on $CeAu_2Si_2$, $CePd_2Si_2$, $CeRh_2Si_2$, and $CeRu_2Si_2$, focussing on the temperature dependence of the quasielastic scattering. Crystal-field splittings will be discussed in a separate paper. In Table I the respective Néel temperatures of the CeX_2Si_2 compounds are listed. $CeAu_2Si_2$ orders antiferromagnetically at $T_N = 10$ K and does not show signs of spin or valence fluctuations.[1] Its ordered magnetic moment determined by neutron diffraction[2] ($\mu_{\mathrm{ord}} = 1.29\mu_B$)

TABLE I. Parameters of CeX_2Si_2, X = Au, Pd, Rh, Ru, and Cu. T_N Néel temperature, T_K Kondo temperature as defined in the text and for Cu the quasielastic linewidth for $T \to 0$ K (Ref. 21), V unit cell volume, a and c lattice parameters, a/c ratio, Ce-X cerium metal distance.

X	T_N (K)	T_K (K)	V (Å^3)	a Ce-Ce (Å)	c (Å)	a/c	Ce-X (Å)
Au	10.0	1.7	190.169	4.32	10.19	0.424	3.400
Pd	10.0	10.0	177.619	4.24	9.88	0.429	3.264
Rh	37.0	33.0	170.619	4.09	10.18	0.402	3.265
Ru		15.0	171.699	4.19	9.78	0.428	3.220
Cu	sc	10.0	167.336	4.103	9.94	0.413	3.222

is smaller than the full Ce^{3+} moment but this can be explained by crystal-field splittings. $CePd_2Si_2$ (Ref. 1) and $CeRh_2Si_2$ (Ref. 3) also order antiferromagnetically (T_N's see Table I) and their transport properties, e.g., resistivity[1,4] and thermopower[5] indicate the presence of spin fluctuations. Furthermore, the ordered magnetic moment of $CePd_2Si_2$ is strongly reduced [$\mu_{ord}=0.62\mu_B$ (Ref. 2)] and its Curie-Weiss temperature is rather large in comparison to the ordering temperature ($\Theta_{CW}=-75$ K).[1] For $CeRh_2Si_2$ the magnetic structure is not uniquely determined, and therefore the ordered magnetic moment of $\mu_{ord}=2.39\mu_B$ (Ref. 2) is doubtful. $CeRu_2Si_2$ exhibits strong valence fluctuations and it does not order magnetically.[6] The bulk susceptibility $\chi_{bulk}(T)$ measured on a $CeRu_2Si_2$ polycrystal shows, Curie-Weiss-like behavior above 50 K but reaches a constant value below 10 K. Susceptibility measurements on a single crystal[7] show that the magnetization is strongly anisotropic, it occurs mainly along the c axis ($\chi_{bulk}\|c \simeq 15\chi_{bulk}\perp c$). In addition $\chi_{bulk}\|c$ exhibits a distinct maximum at 10 K. The linear coefficient γ of the specific heat is strongly enhanced. Reported values for γ are 385, 310, and 360 mJ/mol K^2 (Refs. 8–10), respectively.

EXPERIMENT AND RESULTS

Polycrystaline CeX_2Si_2 (X=Au, Pd, Rh, Ru) samples were prepared by arc melting. X-ray diffraction patterns show that all samples crystallize in the $ThCr_2Si_2$ structure ($I4/mmm$) and that they are single phased. The lattice constants agree with those reported previously.[2,4]

The double differential cross section for paramagnetic scattering, as measured in neutron scattering experiments can be expressed in the following way:

$$d^2\sigma/d\Omega\, d\omega = N|\mathbf{k}_1|/|\mathbf{k}_0| S(Q,\omega) ,$$

where N is the number of magnetic scatterers and $\mathbf{k}_0$ and $\mathbf{k}_1$ are the initial and final neutron wave vector. $S(Q,\omega)$ is the scattering function, related to the imaginary part of the dynamic susceptibility $\chi''(Q,\omega)$ via

$$S(Q,\omega) = A\,[1-\exp(-\hbar\omega/k_BT)]^{-1}\chi''(Q,\omega) .$$

Here $A=1/(2\pi)(g_N r_e/\mu_B)^2$ describes the coupling between the neutron and electron spin whereby $g_N=-1.91$, r_e is the classical electron radius, and μ_B is the Bohr magneton. The Kramers-Kronig relation provides a relationship between $\chi''(Q,\omega)$ and the static susceptibility $\chi(Q)$ which can be written as follows:

$$\chi''(Q,\omega) = \pi\hbar\omega\chi(Q)P(Q,\omega) .$$

The static susceptibility $\chi(Q)$ is related to the bulk susceptibility χ_{bulk} (susceptometer value) via a magnetic form factor $f(Q)$, $\chi(Q)=|f(Q)|^2\chi_{bulk}$. $f(Q)$ includes the local magnetic form factor $F(Q)$ and the $|Q|$ dependence due to magnetic correlations, i.e., in the absence of correlations $f(Q)$ is identical with $F(Q)$. $P(Q,\omega)$ is a spectral function which has to fullfil the normalization condition $\int_{-\infty}^{\infty} P(Q,\omega)d\omega=1$. Describing relaxation processes $P(Q,\omega)$ is usually assumed to be a Lorentzian. For pure quasielastic scattering the Lorentzian line is centered at $\hbar\omega=0$, in the presence of crystal field splittings $P(Q,\omega)$ is described by a series of Lorentzians centered at $\hbar\omega=0$ (quasielastic) and $\pm\hbar\omega_i$ (crystal field excitations). We will show in the following that $P(Q,\omega)$, i.e., $\chi''(Q,\omega)/\omega$ is not always necessarily Lorentzian.

The experiments were performed at the high-flux reactor at the Institüt Laue-Langevin using the time-of-flight (TOF) spectrometer IN6, located at the cold-neutron guide. We used an incident energy of $E_0=3.14$ meV ($\lambda=5.1$ Å). The available energy window is limited by the incident energy for neutron energy loss scattering (positive energy transfers) and by the thermal occupancy on the neutron energy-gain side (negative energy transfers), i.e., with increasing temperature the energy window increases. The instrument was set up for an energy resolution of $\Delta E=45$ μeV (HWHM) at the elastic peak. Background correction was determined by measurements on the empty sample holder and on a cadmium plate in the sample position. The spectra shown are corrected for background scattering, absorption (energy and angle dependent), and detector efficiency and are calibrated to absolute intensities by measurements on a vanadium standard. Furthermore the strong change of the resolution function with energy transfer due to the time focussing on the IN6 spectrometer is taken into account. The statistical error in the spectra is reflected by the scattering among the data points. In order to separate magnetic and phonon scattering a nonmagnetic reference compound, $LaPd_2Si_2$ was measured and the $|\mathbf{Q}|$ dependence of the scattering response was analyzed ($\mathbf{Q}$=momentum transfer). The phonon scattering increases with increasing $|\mathbf{Q}|$, whereas the magnetic scattering follows the local magnetic form factor. From the La sample the $|\mathbf{Q}|$ dependence of the phonon scattering was determined, the $|\mathbf{Q}|$ dependence of the magnetic scattering is given by the well-known local Ce^{3+} magnetic form factor. Fitting the high- and low-$|\mathbf{Q}|$ data of the cerium sample consistently with respect to the La data allows to separate magnetic and phonon scattering. We did not simply subtract the phonon contribution from the magnetic sample because the phonon frequencies vary with differences in the lattice constants and atomic masses. In addition the latter method requires a correction for the different scattering lengths of the constituents. When no $|\mathbf{Q}|$ dependence of the magnetic response other than the local magnetic form factor is observed, the low-angle detectors are grouped together. For the data fits the intensity is divided by the square of the local magnetic form factor for each detector and channel. The detector grouping is limited to a $|\mathbf{Q}|$ range for which phonon scattering does not contribute significantly. In the presence of a $|\mathbf{Q}|$ dependence a constant $|\mathbf{Q}|$ analysis is performed: only time-of-flight channels corresponding to a $|\mathbf{Q}|$ value within a certain window are included in the analysis. The available $|\mathbf{Q}|$ range at low temperatures is 0.5–1.8 Å^{-1}.

$CeAu_2Si_2$ is measured in the temperature range 1.5 K$\le T\le$150 K. No $|\mathbf{Q}|$ dependence of the magnetic response is observed in this range. Therefore, the low-angle detectors are grouped together in order to improve the statistics. Figure 1 shows the 150, 50, and 11 K spec-

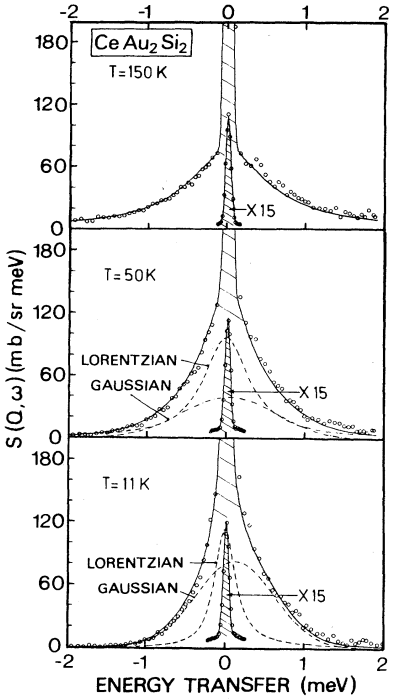

FIG. 1. Quasielastic spectra ($18° \leq 2\Theta \leq 54°$) of $CeAu_2Si_2$ above T_N, at 150, 50, and 11 K. The solid line in the 150 K spectrum represents a single quasielastic Lorentzian fit, in the 50 and 11 K a fit with a quasielastic Lorentzian and a quasielastic Gaussian. There the Lorentzian (dashed line) and Gaussian (dashed dotted line) contributions are shown separately.

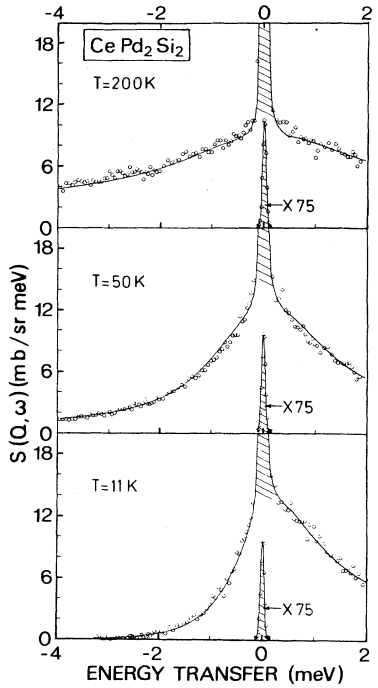

FIG. 2. Quasielastic spectra of $CePd_2Si_2$ ($18° \leq 2\Theta \leq 34°$) above T_N, at 200, 50, and 11 K. The solid lines are single quasielastic Lorentzian fits.

tra of $CeAu_2Si_2$. At 150 K the quasielastic part of the spectrum is well described by a quasielastic Lorentzian of width, $\Gamma/2 = 0.58$ meV (6.7 K). With decreasing temperature the linewidth narrows. For $T_N \leq T \leq 50$ K ($T_N \simeq 10$ K) a single quasielastic Lorentzian line does not yield satisfactory fits. A constant-$|\mathbf{Q}|$ analysis does not improve these fits, however, an additional quasielastic Gaussian gave significant improvement. In Fig. 1 the Lorentzian and Gaussian lines are shown separately by the dashed and dashed-dotted lines. The Gaussian contribution to the quasielastic scattering increases with decreasing temperature, at $T = 11$ K the Gaussian intensity is $I_{\text{Gauss}} = 1.29$ b and the Lorentzian $I_{\text{Lore}} = 0.81$ b. The Gaussian linewidth is larger than the Lorentzian and nearly temperature independent. The resulting linewidths (Lorentzian and Gaussian) are shown in Fig. 5 by the closed and open circles. Below T_N, inelastic scattering due to magnons increases while the quasielastic intensity drops and finally disappears below 3 K (see bottom of Fig. 3). The magnon positions move towards higher energy transfers with decreasing temperature. At high temperatures, crystal-field excitations are observed in energy gain and can be fitted consistently with thermal data.[11]

$CePd_2Si_2$. Figure 2 shows the quasielastic spectra of $CePd_2Si_2$ at several temperatures for a particular detector grouping. Over the whole temperature range the quasielastic part of the spectrum is well described by a quasielastic Lorentzian. In Fig. 5 the quasielastic linewidth versus temperature is shown (triangles). $\Gamma/2$ is larger than in $CeAu_2Si_2$ and increases faster with increasing temperature. At about 10 K, i.e., at the Néel temperature, $\Gamma/2$ becomes as large as the thermal energy ($\Gamma/2 \simeq k_B T_N$), below T_N, the magnetic response behaves as in $CeAu_2Si_2$. The quasielastic intensity drops, and instead inelastic magnon scattering appears (see top of Fig. 3), and the magnon energy increases with decreasing temperature. The magnon scattering occurs at slightly higher energy transfers than in $CeAu_2Si_2$ which may be due to the different magnetic structures.[2] Furthermore the magnon intensity in $CePd_2Si_2$ is weaker than in $CeAu_2Si_2$ (notice the different scales) which is consistent with the differences of the magnetic moments in the magnetically ordered state: $\mu_{\text{ord}}(\text{Au})/\mu_{\text{ord}}(\text{Pd}) \simeq 2.1$ from neutron diffraction experiments[2] and $\mu_{\text{mag}}(\text{Au})/\mu_{\text{mag}}(\text{Pd}) \simeq 1.8$ with μ_{mag} determined from the integrated magnon intensity σ_{mag} at 1.5 K (Fig. 3) ($\sigma_{\text{mag}} = \int d^2\sigma/d\Omega\, d\omega \times d\omega = 0.605$ b$/\mu_B^2 \mu_{\text{mag}}^2$. At high temperatures inelastic magnetic scattering due to crystal-field splitting is observed, and our crystal-field analysis agrees with the results of Ref. 11. It should be mentioned that a slight $|\mathbf{Q}|$ dependence of the quasielastic response above the Néel temperature cannot be excluded. Unfortunately a proper constant $|\mathbf{Q}|$ analysis is prevented by Bragg scattering in some detectors. The quasielastic intensity appears to increase with increasing $|\mathbf{Q}|$ whereas the linewidth decreases. Beyond $|\mathbf{Q}| \simeq 1.2$ Å^{-1} the quasielastic intensity

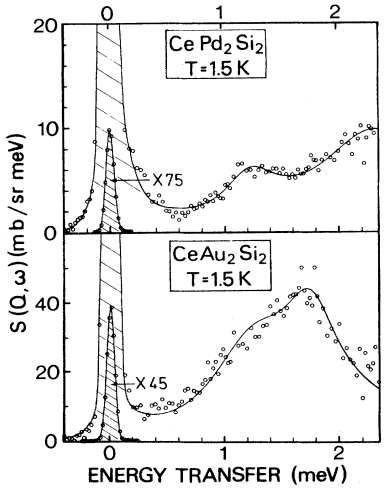

FIG. 3. Magnon scattering of $CeAu_2Si_2$ and $CePd_2Si_2$ at 1.5 K. The solid lines represent a fit with two inelastic Lorentzian peaks.

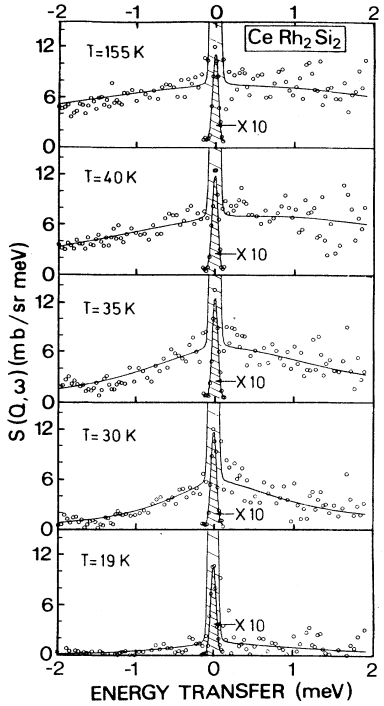

FIG. 4. Quasielastic spectra ($18° \leq 2\Theta \leq 41°$) of $CeRh_2Si_2$ above and below T_N ($T_N = 37$ K). The solid lines are fits with a single quasielastic Lorentzian.

decreases again and the quasielastic width increases. However, the maximum of the quasielastic intensity at $|\mathbf{Q}| = 1.2$ Å^{-1} coincides with the (002) Bragg reflection, i.e., the $|\mathbf{Q}|$ dependence might be due to nuclear scattering.

$CeRh_2Si_2$. The large absorption cross section of Rh ($\simeq$400 b for an energy of 3.14 meV) coupled with a broad magnetic signal is responsible for the poorer quality of the data for the Rh-based sample. Consequently, in order to increase the statistical accuracy of the data, we summed as many detectors as possible. The spectra of $CeRh_2Si_2$ are shown for various temperatures in Fig. 4. The resulting quasielastic linewidths (single Lorentzians) are depicted in Fig. 5 (squares). Above the ordering transition ($T_N = 37$ K) the quasielastic linewidth is larger than for $CePd_2Si_2$. It should be mentioned that due to the large absorption the energy-dependent absorption correction may well be incorrect. With increasing linewidth higher energy transfers have to be taken into account for the fit, and therefore a systematic error in the absorption correction becomes increasingly important. Below T_N (37 K) the quasielastic intensity and linewidth decrease, but at 35 K and still at 30 K a non-negligible amount of quasielastic scattering exists. At $T = 19$ K the quasielastic scattering has already nearly disappeared (see Fig. 4). Neither at 10 K nor at 1.5 K do we observe magnon scattering within the available energy window. The leftover quasielastic intensity at 35 and 30 K might be due to a second-ordering transition at 29 K as observed by neutron diffraction.[2]

$CeRu_2Si_2$ is measured in the temperature interval 1.5 K $\leq T \leq$ 250 K. In contrast to the other compounds the magnetic response of $CeRu_2Si_2$ does show a pronounced $|\mathbf{Q}|$ dependence below 50 K. In addition its ground state shows many interesting properties.

Above 50 K, no $|\mathbf{Q}|$ dependence of the magnetic scattering is detected, therefore, the low-angle detectors were grouped together. As shown in Fig. 6 the quasielastic response broadens significantly between 50 and 250 K. Inelastic magnetic scattering due to crystal-field excitations is not observed, see Ref. 11. For $T \leq 50$ K we observed a distinct $|\mathbf{Q}|$ dependence of the quasielastic magnetic scattering and therefore, a constant $|\mathbf{Q}|$ analysis with $|\mathbf{Q}|$ windows of width 0.2 Å^{-1} is used. The $|\mathbf{Q}|$

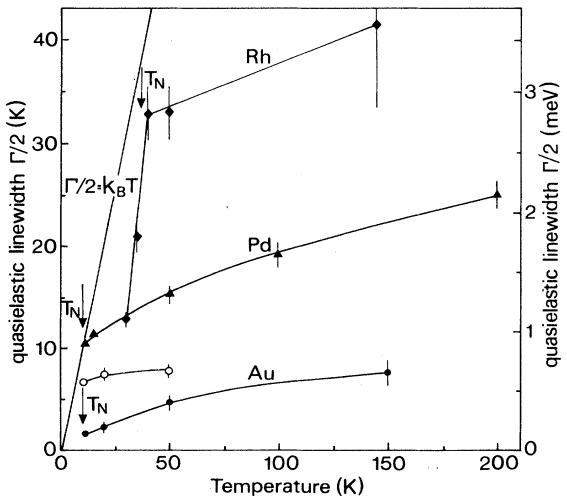

FIG. 5. Quasielastic linewidths vs temperature for $CeAu_2Si_2$ (● Lorentzian, ○ Gaussian), $CePd_2Si_2$ (▲) and $CeRh_2Si_2$ (◆). The arrows indicate the Néel temperatures. The solid lines are guides to the eye.

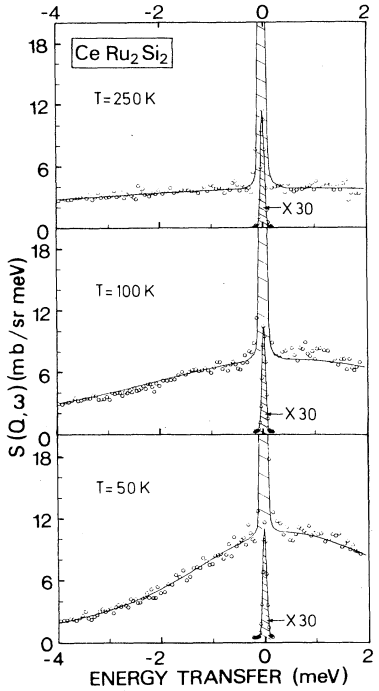

FIG. 6. Quasielastic spectra of $CeRu_2Si_2$ for a particular detector grouping ($22° \leq 2\Theta \leq 39°$) at 250, 100, and 50 K including the fit with a single quasielastic Lorentzian (solid line).

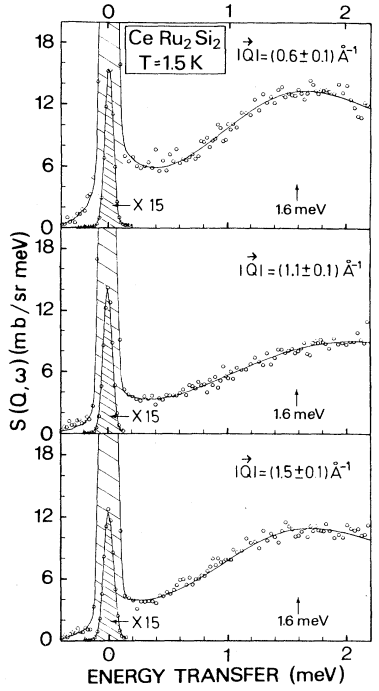

FIG. 7. Magnetic response of $CeRu_2Si_2$ at 1.5 K for three different $|\mathbf{Q}|$ values fitted with an inelastic Lorentzian (solid lines).

dependence of the quasielastic response is demonstrated in Fig. 7 for the 1.5 K spectrum and three different $|\mathbf{Q}|$ windows. The resulting linewidths of a single quasielastic Lorentzian fit are plotted in Fig. 8. At high temperatures the error bars for the linewidths determined from the IN6 data are large because the quasielastic line is rather broad compared to the energy window. However, we could pinpoint the linewidth with the knowledge of the results of 12.5-meV measurements of Rainford *et al.*,[12] and we obtained satisfactory fits. The quasielastic linewidth from Rainford *et al.* are included in Fig. 8 as squares. Although the quality of a quasielastic fit becomes worse with decreasing temperature, we forced a quasielastic Lorentzian fit down to the lowest temperature. For $T \leq 50$ K the quasielastic linewidths are obtained from a constant $|\mathbf{Q}|$ analysis. For all $|\mathbf{Q}|$ values within the available $|\mathbf{Q}|$ range the quasielastic linewidth goes through a minimum at about 20 K and increases upon a further decrease of temperature which is shown in Fig. 8 for $|\mathbf{Q}|=(0.6\pm0.1)$ Å^{-1} and $|\mathbf{Q}|=(1.1\pm0.1)$ Å^{-1}. However, looking at the quasielastic fits at low temperatures in greater detail it becomes apparent that a quasielastic Lorentzian is not appropriate here [see, for example, the quasielastic fit of the 1.5 K spectrum for $|Q|=(0.6\pm0.1)$ Å^{-1} in Fig. 9]. Therefore, we fitted the $CeRu_2Si_2$ spectra for $T < 20$ K with an inelastic Lorentzian line which improved the quality of the fits significantly (see Fig. 9). In contrast to the quasielastic linewidth, the inelastic linewidth $\Gamma_i/2$ decreases with decreasing temperature below 20 K; it actually is a continuation of the quasielastic one (see inset of Fig. 8). The inelastic posi-

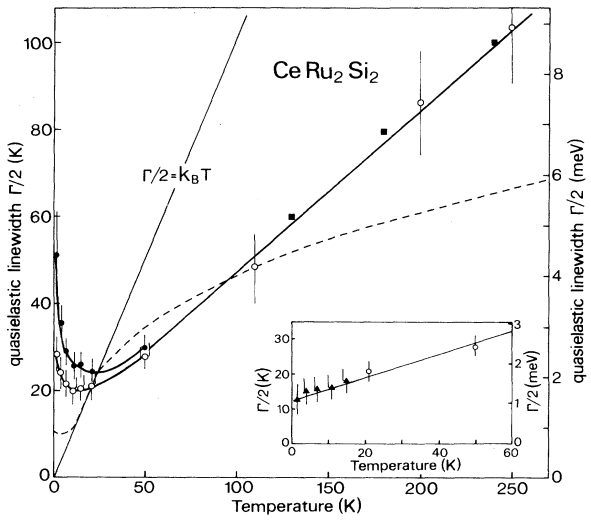

FIG. 8. Quasielastic linewidth of $CeRu_2Si_2$ vs temperature. Above 50 K the detectors were grouped, for $T \leq 50$ K a constant $|\mathbf{Q}|$ analysis was performed: ○, $\Gamma/2$ for $|\mathbf{Q}|=(0.6\pm0.1)$ Å^{-1} and ●, $\Gamma/2$ for $|\mathbf{Q}|=(1.1\pm0.1)$ Å^{-1}. The squares are results of a 12.5-meV measurement by Rainford *et al.* (Ref. 12). The solid lines are guides to the eye, the dashed line scratches the temperature dependence of the quasielastic linewidth of $CeCu_2Si_2$ (Ref. 23). In the inset the inelastic linewidth (▲) resulting from an inelastic Lorentzian fit is shown for $|\mathbf{Q}|=(0.6\pm0.1)$ Å^{-1}. The open circles are quasielastic linewidths (same as in large figure).

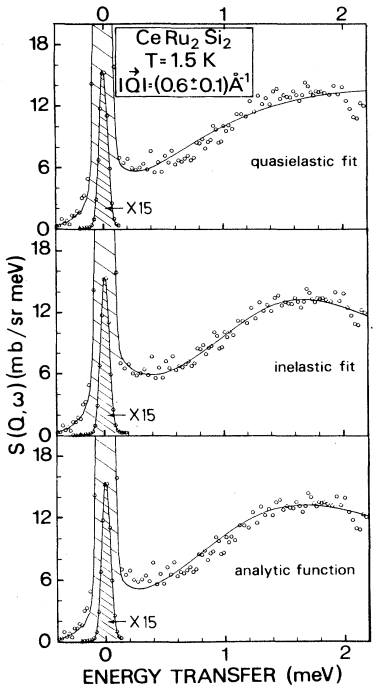

FIG. 9. $CeRu_2Si_2$ spectrum at 1.5 K for $|\mathbf{Q}|=(0.6\pm0.1)$ Å^{-1}, fitted with a quasielastic Lorentzian (top), an inelastic Lorentzian (middle), and an analytic function for $\chi''(\omega)/\omega$ given by Ref. 30 (bottom).

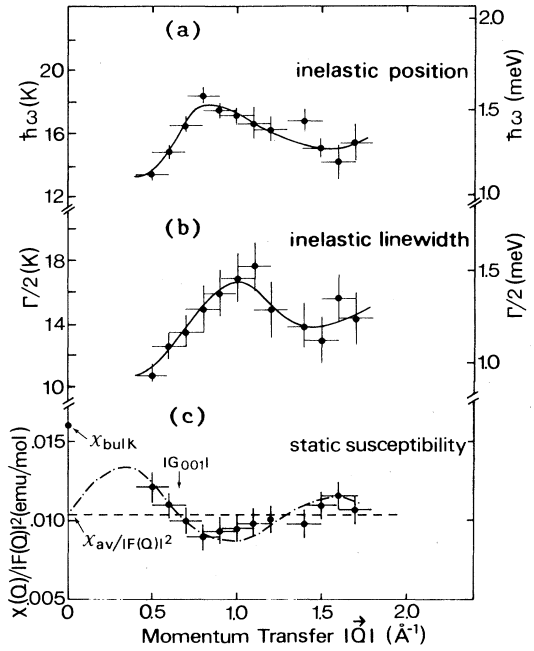

FIG. 10. (a) The inelastic position, (b) the inelastic linewidth, and (c) the static susceptibility divided by the local magnetic form factor are plotted vs $|\mathbf{Q}|$. The values result from an inelastic Lorentzian fit of the 1.5 K spectrum of $CeRu_2Si_2$ (see text). χ_{bulk} indicates the bulk susceptibility as reported in Ref. 6, the dashed-dotted curve represents a guide to the eye.

tion moves from $\hbar\omega_i \simeq 0.48$ meV (5.6 K) for $|\mathbf{Q}|=(0.6\pm0.1)$ Å^{-1} at 15 K towards higher energy transfers with decreasing temperature, and at 1.5 K the inelastic linewidth and position are roughly identical [see Figs. 10(a) and 10(b)]. This applies for all $|\mathbf{Q}|$ values.

Here we will consider the $|\mathbf{Q}|$ dependence of the low-energy excitation in $CeRu_2Si_2$. Powder measurements have the disadvantage that $|\mathbf{Q}|$ dependences with respect to certain crystallographic axis cannot be determined. However, a constant $|\mathbf{Q}|$ analysis of powder data provides the possibility to cut out $|\mathbf{Q}|$ shells of a certain width from the reciprocal space, and if in addition the neutron time-of-flight technique is applied, the whole energy spectrum is measured simultaneously for each $|\mathbf{Q}|$ shell. Therefore (and because of the good energy resolution of IN6), we were able to investigate the $|\mathbf{Q}|$ dependence of the inelastic line shape, i.e., to determine the position $\hbar\omega_i$ and linewidth $\Gamma_i/2$ as function of $|\mathbf{Q}|$ as depicted in Figs. 10(a) and 10(b). The horizontal error bars represent the $|\mathbf{Q}|$ windows. The position $\hbar\omega_i$ and linewidth $\Gamma_i/2$ of the inelastic Lorentzian line are modulated in $|\mathbf{Q}|$ whereas the intensity turns out to be constant within the error bars. In Fig. 10(c) the static susceptibility $\chi(\mathbf{Q})$ divided by the squared local magnetic form factor $F(Q)$ is plotted versus $|\mathbf{Q}|$. $\chi(Q)/|F(Q)|^2$ varies around an average value $\chi_{av}(Q)/|F(Q)|^2$ which is indicated by the horizontal dashed line.

Antiferromagnetic correlations imply $\chi(Q)/|F(Q)|^2$ to be smallest for $|\mathbf{Q}|=0$, i.e., for the bulk value $[\chi(Q=0)=\chi_{bulk}$ and $F(Q=0)=1]$. However, here the bulk susceptibility taken from Ref. 6 is larger than the susceptibility values at finite $|\mathbf{Q}|$ [see χ_{bulk} in Fig. 10(c)] but an interpretation in terms of ferromagnetic correlations would be in disagreement with the static (bulk) susceptibility.[6] However, the integrated magnetic intensity $\sigma_{mag}(Q)$ yields about 1.3 b ($\pm15\%$) which is by factor of $\simeq 3$ less than the full Ce^{3+} magnetic cross section. The latter suggests the existence of additional magnetic intensity which has not been observed yet.[11] From the crystal-field analysis of the CeX_2Si_2 series[11] we know that the contribution of van Vleck terms to the total static susceptibility is about 30%. Adding to $\chi_{av}(Q)/|F(Q)|^2$ in $CeRu_2Si_2$ a van vleck susceptibility due to crystal-field excitations of $\simeq 30\%$ of χ_{bulk}, shifts $\chi(Q=0)/|F(Q=0)|^2$ up to the bulk value.

In the following our results shall be compared with $CeRu_2Si_2$ single-crystal data of Erkelens *et al.*[13] The $|\mathbf{Q}|$ modulation of the inelastic linewidth and position was not observed in the single-crystal experiment.[13] Erkelens *et al.* performed Q scans at a given energy transfer ($\hbar\omega$=const=1.6 meV, see arrows in Fig. 7) along the ⟨100⟩ and ⟨110⟩ direction, i.e.., the neutron count rate at a given energy transfer was measured as function of Q. This provides information neither about the line shape nor about the integrated magnetic cross section or the static susceptibility. They observed a strong-Q modulation of the count rate along the two symmetry directions

as shown in Figs. 11(a) and 11(b) (in Fig. 11 $|\mathbf{Q}|$ is plotted instead of $\mathbf{Q}$). The vertical dashed lines in Fig. 11 indicate characteristic points in the reciprocal space. The first minimum (maximum) in the count rate in Fig. 11 corresponds to the maximum (minimum) in the inelastic position and linewidth in Fig. 10. It shall be shown that the $|\mathbf{Q}|$ modulation of the position and linewidth cause the $|\mathbf{Q}|$ dependence of the count rate at 1.6 meV. We calculated the intensity $I(|\mathbf{Q}|,\hbar\omega)$ of the inelastic Lorentzian line at the energy transfer $\hbar\omega=1.6$ meV via

$$I(|\mathbf{Q}|,\hbar\omega)=\langle A\rangle\frac{\Gamma_i(|\mathbf{Q}|)/2}{[\Gamma_i(|\mathbf{Q}|)/2]^2+[\hbar\omega_i(|\mathbf{Q}|)-\hbar\omega]^2}$$

using the $|\mathbf{Q}|$-dependent linewidth $\Gamma_i(|\mathbf{Q}|)/2$ and peak centers $\hbar\omega_i(|\mathbf{Q}|)$ from Figs. 10(a) and 10(b). $\langle A\rangle$ is the $|\mathbf{Q}|$-averaged amplitude. The resulting $|\mathbf{Q}|$ dependence of the intensity $I(|\mathbf{Q}|, \hbar\omega=1.6$ meV) reproduces the count rates of the single-crystal data [see Fig. 11(c)].

Triple-axis data of $CeAu_2Si_2$, $CePd_2Si_2$, and $CeRu_2Si_2$ powders taken by Grier *et al.*[14] are in agreement with our results. The authors of Ref. 14 did not interpret their low-temperature $CeRu_2Si_2$ data in terms of an inelastic line, but this can be understood by the poorer energy resolution and quality of the powder triple-axis data.

DISCUSSION

The quasielastic response of the compounds CeX_2Si_2 with $X=$Au, Pd, Rh, and Ru has been studied as function of temperature. The weak local $4f$ conduction electron exchange in $CeAu_2Si_2$ manifests itself in a narrow quasielastic linewidth and well-established crystal-field excitations. A Gaussian contribution to the quasielastic response starts to develop at temperatures which are about five times larger than T_N. The Gaussian spectral weight increases with decreasing temperature until the ordering transition is reached. This effect has already been observed in other magnetically ordering compounds like YbPd, Yb_3Pd_4 (Ref. 15), UBe_{13} (Ref. 16), U_2Zn_{17}, UCu_5 (Ref. 17), CeInAu (Ref. 18), and $YbAuCu_4$ (Ref. 19). In Refs. 15–17, this phenomenon is interpreted as enhanced spin fluctuations preceding a magnetic ordering transition. For the latter reason, i.e., because we attribute the Gaussian line to the magnetic ordering, we consider only the Lorentzian linewidth as a representative value for the strength of the $4f$ conduction-electron scattering. At the ordering temperature the quasielastic Lorentzian linewidth is smaller than $k_BT_N(\Gamma/2\simeq 0.17k_BT_N)$, i.e., in $CeAu_2Si_2$ the Kondo temperature T_K is smaller than the Néel temperature ($T_N\gg T_K$) if one identifies the value $\Gamma/2k_B$ at $T=T_N$ with the Kondo temperature T_K ($\Gamma/2=$Lorentzian quasielastic linewidth). Hence, in $CeAu_2Si_2$ the RKKY interaction exceeds the local $4f$ conduction-electron scattering and magnetic order can develop.

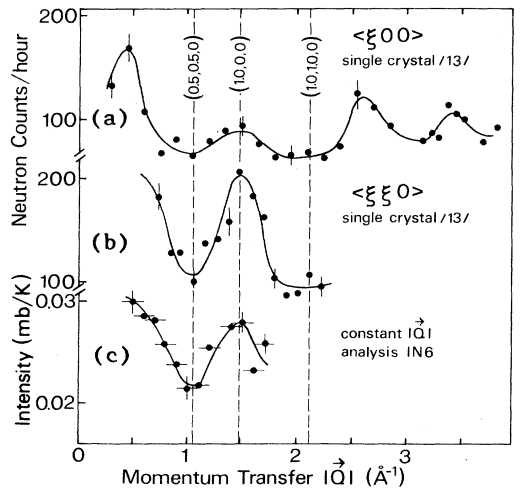

FIG. 11. Count rate at 1.6 meV vs $|\mathbf{Q}|$ from $CeRu_2Si_2$ single-crystal measurements (Ref. 13) (a) along the ⟨100⟩ and (b) along the ⟨110⟩ direction. (c) Intensity of the inelastic Lorentzian at 1.6 meV resulting from the constant $|\mathbf{Q}|$ analysis of the powder data.

In $CePd_2Si_2$ the broader quasielastic linewidth as well as the broadened crystal-field excitations imply a stronger local $4f$ conduction-electron scattering. $\Gamma/2$ increases faster with temperature as in $CeAu_2Si_2$. At the ordering transition, $\Gamma/2$ is as large as the thermal energy, i.e., Kondo and Néel temperature are comparable ($T_N\simeq T_K$). Although the RKKY interaction succeeds at low temperatures, the ordered magnetic moment is strongly reduced, i.e., a significant Kondo screening by $4f$ exchange scattering is still present in the ordered state. A Gaussian quasielastic line has not been observed, possibly because the RKKY interaction is too weak.

For $CeRh_2Si_2$ it is unclear where in the sequence it has to be placed. The quasielastic linewidth of $CeRh_2Si_2$ is larger than in $CePd_2Si_2$ suggesting a stronger $4f$ exchange coupling. On the other hand, its Néel temperature is 3.7 times larger than in $CeAu_2Si_2$ and $CePd_2Si_2$ (for Rh, $T_N=37$ K). The latter leads to the assumption of a stronger RKKY interaction. At $T=T_N$ the quasielastic linewidth is smaller than the thermal energy ($\Gamma/2\simeq 0.8k_BT_N$), i.e., $T_N>T_K$. All this suggests that in $CeRh_2Si_2$ both processes are stronger, more so in $CePd_2Si_2$ but that the relative strength of the $4f$ exchange coupling is weaker than in $CePd_2Si_2$.

For $CeRu_2Si_2$ we assume a hypothetical Néel temperature of $T_N^{\rm hyp}\simeq 10$ K. This assumption is justified because $CeRu_2Si_{2-x}Ge_x$ orders magnetically for $x\geq 0.5$ at about 10 K (Ref. 20). In $CeRu_2Si_2$ the linewidth is largest. At $T=T_N^{\rm hyp}$ the linewidth is larger than $k_BT_N^{\rm hyp}$, i.e., the local $4f$ conduction-electron scattering is so strong that the magnetic order becomes suppressed ($T_N\ll T_K$).

The sequence can be understood if one considers that with increasing pressure on the cerium (chemical or physically applied), the Kondo temperature T_K increases relative to the Néel temperature T_N since T_K depends exponentially on the exchange parameter, while the RKKY interaction increases quadratically.[21,22] In Fig. 12 T_K and $T_{\rm RKKY}$ (measure of the RKKY interaction) are shown as a function of the normalized exchange parameter J. The solid line shows the qualitative dependence of the magnetic ordering temperature T_M (here $T_M=T_N$)

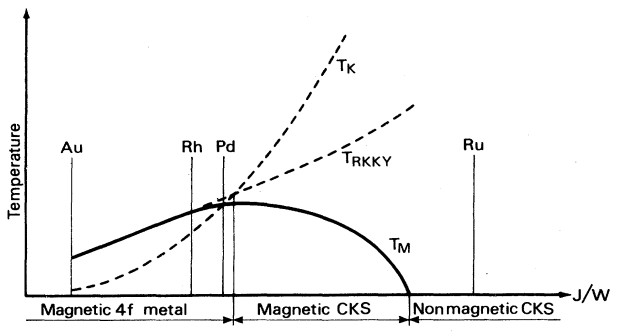

FIG. 12. The classification of the condensed Kondo systems (CKS) by the relation between two characteristic temperatures T_K and T_{RKKY}. T_M is the magnetic ordering temperature (here $T_M = T_N$), J is the $4f$ exchange integral, and W is a scaling factor. (Taken from Ref. 22).

on the ratio of T_K and T_{RKKY}. For $T_{RKKY} \gg T_K$ the RKKY interaction dominates, and these compounds represent ordinary magnetically ordered $4f$ metals. In the intermediate situation $T_{RKKY} \leq T_K$ the magnetic ordering temperature does not increase with T_{RKKY}, it is reduced due to the $4f$ instability of the $4f$ moments. With further increasing J the local $4f$ conduction-electron scattering dominates, and magnetic order is destroyed. In Fig. 12 the positions of the CeX_2Si_2 compounds are qualitatively determined from the ratios T_K/T_N (see T_K and T_N in Table I). It is intriguing that $CeAu_2Si_2$ exhibits the full Ce^{3+} moment in the ordered state, whereas the ordered magnetic moment of $CePd_2Si_2$ is reduced.

The sequence is supported by the unit cell volumes of the CeX_2Si_2. In Table I the unit cell volumes V are listed. Ignoring $CeRh_2Si_2$ for the moment, the unit cell volumes decrease from $CeAu_2Si_2$ to $CeRu_2Si_2$, i.e., the pressure on the cerium increases, thus explaining the increasing relative and absolute strength of the local $4f$ exchange coupling from $CeAu_2Si_2$ to $CeRu_2Si_2$ (see Fig. 12). The substitution of Si by Ge in $CeRu_2Si_2$ expands the compound chemically so that $CeRu_2Si_{2-x}Ge_x$ orders magnetically above a certain x value. $CeRh_2Si_2$ does not fit into the series: its unit cell volume is smaller than in $CeRu_2Si_2$. From this point of view $CeRh_2Si_2$ should not order magnetically, however, it exhibits the highest-ordering temperature. On the other hand, the unit cell volume of $CeRh_2Si_2$ is smaller than in $CePd_2Si_2$, implying the ratio T_K/T_N to increase with respect to $CePd_2Si_2$, however, T_K/T_N is smaller than in $CePd_2Si_2$. The stronger anisotropy of the $CeRh_2Si_2$ lattice might explain the puzzle. In Table I the lattice constants a and c (a is also the next-nearest cerium-cerium distance) and the ratios a/c are also listed. For the X = Au-, Pd-, and Ru-based samples the a/c ratios are nearly identical whereas a/c is distinctively smaller for $CeRh_2Si_2$, showing that in $CeRh_2Si_2$ the next-nearest cerium-cerium distance is rather small whereas the c parameter is rather large. The latter leads to a next-nearest cerium-metal distance (Ce-x) which is larger in $CeRh_2Si_2$ than in $CeRu_2Si_2$ (see Table I). The cerium and the transition metals contribute to the conduction-electron band, hence, the Ce-Ce as well as the Ce-X distance influence the exchange interaction.

The dependence of the Néel temperatures on externally applied pressure supports our $CeAu_2Si_2$ and $CePd_2Si_2$ results.[4] The Néel temperature of $CeAu_2Si_2$ remains nearly constant up to pressures of about 15 kbar, i.e., the magnetically ordered state is fairly stable in agreement with $T_N \gg T_K$. In $CePd_2Si_2$ the Néel temperature at 15 kbar is reduced by a factor of 0.6 with respect to the 0 kbar value, which confirms $T_N \simeq T_K$. The magnetic order of $CeRh_2Si_2$ can be suppressed completely, applying a pressure of about 8 kbar only, i.e., the relative strength of RKKY interaction and $4f$ conduction-electron exchange is shifted to the advantage of the latter. However, the upper Rh result, $T_N > T_K$ rather suggests a weaker pressure sensitivity of T_N than in $CePd_2Si_2$ ($T_N \simeq T_K$), although a stronger dependence than in $CeAu_2Si_2$ ($T_N \gg T_K$) (see Fig. 12). Here the small a/c ratio might be responsible again: The stronger crystallographic anisotropy might cause an anisotropy of the pressure dependence of T_N in $CeRh_2Si_2$. Therefore it would be interesting to repeat the same pressure experiment as in Ref. 4 on a single crystal.

Here the results of $CeRu_2Si_2$ (especially the low-temperature results) shall be discussed in greater detail. The quasielastic line of $CeRu_2Si_2$ is very broad, above 100 K $\Gamma/2$ is larger than the quasielastic linewidth of $CeCu_2Si_2$.[23] $\Gamma/2$ decreases with temperature without following a $T^{1/2}$ law which is observed in some heavy-fermion cerium compounds as for example in $CeCu_2Si_2$ (see dashed line in Fig. 8), $CeAl_3$, and $CeCu_6$.[23–26] In $CeRu_2Si_2$, $\Gamma/2$ decreases linearly with temperature (see Fig. 8). In contrast to our results Erkelens *et al.*[13] determined a $T^{1/2}$ behavior from their single-crystal data. However, 90 K is the highest temperature the authors of Ref. 13 measured in contrast to the present 250 K and furthermore, their data do not exclude a linear slope of $\Gamma/2$. In addition, it should be mentioned that in the absence of a $\mathbf{Q}$ dependence (here valid for $T > 50$ K) the quality of TOF powder data is usually better. Below 20 K the magnetic response becomes inelastic, in agreement with Ref. 13. Crystal-field excitations can be excluded as the cause of the inelastic feature at low temperature since every crystal-field scheme requires a minimum quasielastic spectral weight of about 1 b which is not present in $CeRu_2Si_2$ at low temperatures. Furthermore, the crystal-field splittings of the CeX_2Si_2 series [X = Au, Ag, Pd (Ref. 11), Cu (Ref. 23)] are larger by about a factor of 20. Therefore, we exclude the possibility that the inelastic magnetic response observed at low temperatures is a crystal-field excitation. It has to reflect the ground-state properties of $CeRu_2Si_2$. The position of the inelastic line, although $|\mathbf{Q}|$ dependent, coincides roughly with the maximum in the static susceptibility and with a maximum in the specific heat at 11 K which is interpreted as being due to the Kondo effect.[9] A deviation of the magnetic neutron scattering response $\chi''(\omega)/\omega$ from a quasielastic Lorentzian line shape at low temperatures has already

been observed in several compounds[27] and is predicted by several theories. In the following, some of these theories, based on the Anderson model in the $U\rightarrow\infty$ limit ($U=4f$-$4f$ Coulomb repulsion) shall be sketched and compared with the $CeRu_2Si_2$ results.

Cox, Bickers, and Wilkins[28] have calculated the dynamic susceptibility $\chi''(\omega)$ for a cerium impurity for a large temperature interval ($0.01T_0<T<40T_0$). At high temperatures $\chi''(\omega)/\omega$ has a conventional quasielastic Lorentzian line shape and below a certain temperature T_0 (T_0 is the position of the Kondo resonance), the line shape is strongly non-Lorentzian. The calculations yield the following temperature behavior of the quasielastic linewidth if a Lorentzian line shape is assumed: $\Gamma/2$ is roughly constant at low temperatures, goes through a minimum at T_0, and increases monotonically above $T=T_0$, finally following a $T^{1/2}$ law. The minimum in $\Gamma/2$ at $T=T_0$ indicates the deviation from a Lorentzian line shape below that temperature. In Fig. 8 the linewidth of $CeRu_2Si_2$ is shown resulting from a quasielastic Lorentzian fit. The quasielastic $\Gamma/2$ exhibits a distinct minimum at 20 K. We mentioned before that below 20 K the magnetic response is better fitted with an inelastic line (see Fig. 9 and inset of Fig. 8), i.e., the minimum in $\Gamma/2$ coincides indeed with a deviation from a quasielastic Lorentzian line shape. However, above the minimum temperature the quasielastic linewidth does not follow a $T^{1/2}$ law within the temperature interval measured.

Schlottmann[29] calculated the dynamic susceptibility $\chi''(\omega)$ for an intermediate-valent impurity, applying Mori's formalism. $\chi''(\omega)/\omega$ has a quasielastic Lorentzian shape at high temperatures but exhibits an inelastic excitation at low temperatures. At low temperatures a quasielastic contribution remains, but its intensity has decreased with temperature and its form may deviate from a Lorentzian line shape. The inelastic position $\hbar\omega_i$ corresponds roughly to the promotion energy of an $4f$ electron into the conduction band. The inelastic line is rather broad due to the finite lifetime of the $4f$ level. The inelastic feature is not visible at high temperatures since for $k_BT>\Delta E$ thermal fluctuations smear out the energy difference ΔE. The spin-relaxation rate, i.e., the quasielastic linewidth is nearly temperature independent for $k_BT>\Delta E$, goes through a smooth maximum at $T\simeq\Delta E$, and reaches a finite value for $T\rightarrow 0$ K. The static susceptibility $\chi_{\rm stat}$ shows the same threshold behavior as $\chi''(\omega)$: The low-temperature static susceptibility is of van Vleck type and finite for $T\rightarrow 0$ K (singlet ground state) whereas at high temperatures, when all levels are equally populated, the static susceptibility behavior is Curie-Weiss-like. At intermediate temperatures, i.e., at $k_BT_{\rm max}\simeq\Delta E$ the static susceptibility shows a maximum caused by the beginning population of the higher-lying multiplet. We now compare Schlottmann's results with the $CeRu_2Si_2$ data, neglecting the $|\mathbf{Q}|$ dependence of the scattering response. The $|\mathbf{Q}|$-averaged position of the inelastic Lorentzian line $\hbar\omega_i$ is about 1.38 meV (16 K) [see Fig. 10(a)], i.e., at $T=1.5$ K the Bose factor $1/[\exp(\hbar\omega_i/k_BT)-1]$ is about zero. Therefore, at $T=1.5$ K the ground state is reflected. Following Schlottmann's theory this determines ΔE to be about 1.38 meV (16 K). At $T\simeq 20$ K the Bose factor becomes unity, which is consistent with the observation that above $T\simeq 20$ K the $CeRu_2Si_2$ data can be fitted with a single quasielastic Lorentzian, i.e., the higher-lying multiplet is completely populated by the thermal energy. In contrast to Schlottmann's calculations the quasielastic linewidth of $CeRu_2Si_2$ does show a strong temperature dependence. The dominant contribution of the static susceptibility ($\chi_{\rm stat}\|c$) of $CeRu_2Si_2$ exhibits a maximum at $T_{\rm max}\simeq 10$ K, i.e., $k_BT_{\rm max}\simeq\Delta E$ applies.

Kuramoto and Müller-Hartmann[30] obtained an analytic function for the dynamic susceptibility at zero temperature based on a $1/N$ expansion (N = degeneracy of the ground state). Their expression for $\chi''(\omega)/\omega$ yields an asymmetric line shape, namely,

$$\chi''(\omega)/\omega = C\frac{N}{\pi}\frac{\omega}{(\Delta E)^2}\frac{\sin(\pi\alpha)}{u^2(u^2+4\sin^2\pi\alpha)} \times\left\{\sin(\pi\alpha)\ln[(1-u^2)^2+4u^2\sin^2(\pi\alpha)] +|u|\left[\frac{\pi}{2}-\tan^{-1}\left(\frac{1-u^2}{2|u|\sin(\pi\alpha)}\right)\right]\right\}, \quad (1)$$

where C is the Curie constant and $u=\omega/\Delta E$. α is the ratio of the $4f$ occupancy n_f to the degeneracy N of the ground state ($\alpha=n_f/N$). For $\Delta E+\ln(\Delta E)\gg 1$, ΔE represents the position of the renormalized $4f$ level relative to the Fermi level in analogy to Schlottmann's interpretation. If $\Delta E+\ln(\Delta E)\ll -1$, ΔE is closely related to the Kondo temperature (see Gunnarson and Schönhammer[31]). The degree of asymmetry depends on α and ΔE. For $n_f=1$, given ΔE and if the ground state is a doublet ($N=2$, i.e., $\alpha=0.5$) the line shape is nearly a quasielastic Lorentzian with linewidth ΔE. With increasing degeneracy of the ground state the function becomes increasingly asymmetric and for large enough N it peaks at about ΔE. Schmidt[32] modified the model of Kuramoto and Müller-Hartmann taking crystal-field splittings into account. The Curie part of the dynamic susceptibility leads essentially to the same result as Eq. (1), i.e., Eq. (1) is still applicable in the presence of crystal-field splittings. We applied a least-square fit using the upper expression of $\chi''(\omega)/\omega$ to the $CeRu_2Si_2$ data at $T=1.5$ K because here the zero-temperature limit is already reached. α, ΔE, and an intensity parameter which includes C were varied. Kuramoto and Müller-Hartmann have pointed out that their approximation is only valid for $\hbar\omega>\Delta E$. Near $\hbar\omega=0$ the analytic result underestimates the exact Bethe-ansatz result by about 20%. Therefore we excluded the $\hbar\omega=0$ region from the fitting area. The resulting fits are satisfactory except at small energy transfers. In the bottom part of Fig. 9 a fit of the 1.5 K spectrum for $|\mathbf{Q}|=(0.6\pm 0.1)$ Å^{-1} is shown. The deviation of the fit from the data points at small energy transfers is within the error given by the authors of Ref. 30. The fit yields $\Delta E\simeq 1.38$ meV (16 K) for $|\mathbf{Q}|=(0.6\pm 0.1)$ Å^{-1}, the $|\mathbf{Q}|$-averaged value for ΔE is about 1.6 meV (19 K). This

value is close to the value obtained from Schlottmann's model. The fitted α is 0.26 (± 0.05) which corresponds for $n_f = 1$ to a degeneracy of 3.85 (± 0.74), i.e., the degeneracy of the ground state is smaller than the maximum value of a $J = \frac{5}{2}$ state ($N_{\max} = 6$). For different $|\mathbf{Q}|$ values α and hence the degeneracy N does not change within the error bars. The quartet ground state, resulting from the upper fit may be due to crystal-field splittings with a ground state and first-excited doublet which are nearly degenerate. Therefore, the quartet ground state implies the presence of crystal-field splittings in $CeRu_2Si_2$ in agreement with specific-heat data[9] and ultrasonic data.[33] The latter is supported by the fact that neither a quasielastic, an inelastic, or an analytic function provide sufficient intensity ($\mu_{\text{quasi}} \simeq \mu_{\text{inel}} \simeq \mu_{\text{KMH}} \simeq 1.48\mu_B$) in order to reproduce the magnetic moment as determined from the high-temperature slope of the static susceptibility ($\mu = 2.38\mu_B$) which is nearly the full Ce^{3+} moment of $2.54\mu_B$.

Gunnarson and Schönhammer[31] present a model for $\chi''(\omega)$ including crystal-field and spin-orbit splittings, also applying a $1/N$ expansion. They consider cubic symmetry and take into account the crystal-field splitting into Γ_7 and Γ_8 states for $J = \frac{5}{2}$. The resulting dynamic susceptibility exhibits instead of the crystal-field excitation at E_{CF} an inelastic peak located at $\hbar\omega_i = E_{\text{CF}} + k_B T_K$, where T_K represents the Kondo temperature. In the absence of crystal-field splittings the model is similar to Kuramoto's and Müller-Hartmann's result.

CONCLUSION

The temperature dependence of the quasielastic linewidths of $CeAu_2Si_2$, $CePd_2Si_2$, $CeRh_2Si_2$, and $CeRu_2Si_2$ has been determined. The materials are classified as magnetically ordering $4f$ metal ($CeAu_2Si_2$), as magnetically ordering Kondo compounds ($CeRh_2Si_2$, $CePd_2Si_2$), and as nonordering Kondo or intermediate-valent compound ($CeRu_2Si_2$) by the relation of the characteristic temperatures T_K and T_N. The inelastic magnetic response of $CeRu_2Si_2$ at low temperatures has been discussed in terms of various theoretical approaches. The $|\mathbf{Q}|$ dependence of the low-temperature magnetic response of $CeRu_2Si_2$ leads to a $|\mathbf{Q}|$-dependent static susceptibility.

ACKNOWLEDGMENTS

We wish to thank H. Schmitt from the University of Cologne and C. Freiburg and W. Reichert from the KFA Jülich for the sample preparation and characterization. Furthermore we thank P. Thalmeier and A. P. Murani for helpful discussions. The present work was financially supported by the Deutsche Forschungs Gemeinschaft through Sonderforschungsbereich (SFB) 125 and the Bundes Ministerium für Forschung und Technologie.

[1] V. Murgai, S. Raan, L. C. Gupta, and R. D. Parks, in *Valence Instabilities,* edited by P. Wachter and H. Boppart (North-Holland, Amsterdam, 1982), p. 537.
[2] B. H. Grier, J. M. Lawrence, V. Murgai, and R. D. Parks, Phys. Rev. B **29**, 2664 (1984).
[3] C. Godart, L. C. Gupta, and M. F. Ravet-Krill, J. Less. Common Met. **94**, 187 (1983).
[4] J. D. Thompson, R. D. Parks, and H. Borges, J. Magn. Magn. Mat. **54-57**, 377 (1986).
[5] A. Amato and J. Sierro, J. Magn. Magn. Mat. **47&48**, 526 (1985).
[6] L. C. Gupta, D. E. MacLaughlin, Cheng Tien, C. Godart, M. A. Edwards, and R. D. Parks, Phys. Rev. B **28**, 3673 (1983).
[7] J. Flouquet, P. Haen, F. Lapierre, D. Jaccard, and G. Remenyi, J. Magn. Magn. Mat. **54-57**, 322 (1986).
[8] J. D. Thompson, J. O. Willis, C. Godart, D. E. MacLaughlin, and L. C. Gupta, J. Magn. Magn. Mat. **47&48**, 281 (1985).
[9] M. J. Besnus, J. P. Kappler, P. Lehmann, and A. Mayer, Solid State Commun. **55**, 779 (1985).
[10] F. Steglich, U. Rauchschwalbe, U. Gottwick, H. M. Mayer, G. Sporn, N. Grewe, U. Poppe, and J. J. M. Franse, J. Appl. Phys. **57**, 3054 (1985).
[11] A. Severing, E. Holland-Moritz, B. Rainford, S. Culverhouse, and B. Frick, Phys. Rev. B **39**, 2557 (1989).
[12] B. D. Rainford and S. R. Culverhouse (unpublished results).
[13] W. A. C. Erkelens, Ph.D. thesis, Rijksuniversiteitte Leiden, 1987.
[14] B. H. Grier, J. M. Lawrence, S. Horn, and J. D. Thompson, J. Phys. C **21**, 1099 (1988).
[15] U. Walter and D. Wohlleben, Phys. Rev. B **35**, 3576 (1987).
[16] U. Walter, Z. Fisk, and E. Holland-Moritz, J. Magn. Magn. Mat. **47&48**, 159 (1985).
[17] U. Walter, M. Loewenhaupt, E. Holland-Moritz, and W. Schalbitz, Phys. Rev. B **36**, 1981 (1987).
[18] A. Severing, E. Holland-Moritz, and D. Wohlleben (unpublished).
[19] A. Severing, A. P. Murani, J. D. Thompson, and Z. Fisk (unpublished).
[20] C. Godart, A. M. Umarji, L. C. Gupta, and R. Vijayaraghavan, J. Magn. Magn. Mat. **63&64**, 326 (1987).
[21] S. Doniach, in *Valence Instabilities and Related Narrow Band Phenomena,* edited by R. D. Parks (North-Holland, Amsterdam, 1977), p. 196.
[22] N. B. Brand and V. V. Moshcahlkov, Adv. Phys. **33**, 373 (1984).
[23] S. Horn, E. Holland-Moritz, M. Loewenhaupt, F. Steglich, H. Scheuer, A. Benoit, and J. Flouquet, Phys. Rev. B **23**, 3171 (1981).
[24] A. P. Murani, K. Knorr, K. H. J. Buschow, A. Benoit, and J. Flouquet, Solid State Commun. **36**, 523 (1980).
[25] U. Walter, Z. Phys. B **62**, 325 (1986).
[26] S. M. Shapiro, Physica **136B**, 365 (1986), and references therein.
[27] A. P. Murani, Phys. Rev. B **36**, 5705 (1987), and references therein.
[28] D. L. Cox, N. E. Bickers, and J. W. Wilkins, J. Magn. Magn.

Mat. **54-57**, 333 (1986); N. E. Bickers, D. L. Cox, and J. W. Wilkins, Phys. Rev. B **36**, 2036 (1987).

[29]P. Schlottmann, in *Valence Instabilities,* edited by P. Wachter and B. Boppart (North-Holland, Amsterdam, 1982), p. 471; Phys. Rev. B **25**, 2371 (1982); **29**, 4468 (1984).

[30]Y. Kuramoto and E. Müller-Harmann, J. Magn. Magn. Mat. **52**, 122 (1985).

[31]O. Gunnarson and K. Schönhammer, J. Magn. Magn. Mat. **52**, 227 (1985).

[32]H. J. Schmidt, Ph.D. thesis, University of Cologne, 1988.

[33]D. Weber and B. Luethi (unpublished results).

[34]B. Lloret, B. Chevalier, B. Buffat, J. Etourneau, S. Quezel, A. Lamharrar, J. Rossat-Mignod, R. Calemczuk, and E. Bonjour, J. Magn. Magn. Mat. **63&64**, 85 (1987).